14th International Conference on Structural Safety and Reliability - ICOSSAR'25
1-6 June, 2025 - Los Angeles California, USA
R. Ghanem, E. Johnson, S. Masri and A. Olivier (Eds)

STOCHASTIC MODELING AND SENSITIVITY ANALYSIS FOR SEISMIC RESPONSE IN BRIDGE STRUCTURES

JUNGHO KIM[1] AND ZIQI WANG[2]

[1]University of California, Berkeley
Davis Hall, Berkeley, CA 94720, USA
junghokim@berkeley.edu

[2]University of California, Berkeley
Davis Hall, Berkeley, CA 94720, USA
ziqiwang@berkeley.edu

Key words: Bridge Response, Dimensionality Reduction, Global Sensitivity Analysis, Stochastic Simulation, Uncertainty Quantification.

Abstract. The seismic performance of bridge structures is governed by high-dimensional uncertainties stemming from ground motion variability and structural parameter uncertainties. This paper presents a stochastic modeling framework for forward uncertainty quantification (UQ) and global sensitivity analysis (GSA) of bridge seismic responses. The proposed approach integrates physics-based dimensionality reduction with multivariate conditional distribution modeling to efficiently propagate uncertainties through nonlinear response history analyses (NLRHA). The framework's performance is demonstrated through a case study on the Auburn Ravine bridge model. Results indicate that the stochastic simulator achieves high accuracy while reducing computational cost compared to conventional methods. Variance-based sensitivity analysis reveals that ground motion uncertainties account for more than 60% of the response variability. The framework offers a practical and computationally efficient tool for seismic UQ and sensitivity analysis of bridge structures.

1 INTRODUCTION

The seismic response of bridge structures is influenced by two primary sources of uncertainty: aleatory uncertainties arising from ground motion variability and epistemic uncertainties associated with structural properties. Accurately quantifying these uncertainties is essential for risk-informed design and performance-based seismic engineering [1,2]. However, traditional uncertainty quantification (UQ) methods relying on Monte Carlo simulation (MCS) with nonlinear response history analysis (NLRHA) become computationally prohibitive in high-dimensional input spaces [3,4]. The general NLRHA model is expressed as:

$$\boldsymbol{Y} = \mathcal{M}_{NLRHA}(\boldsymbol{X}) \tag{1}$$

where $\boldsymbol{X} \in \mathbb{R}^n$ is the input vector, $\boldsymbol{Y} \in \mathbb{R}^m$ is the output vector (e.g., engineering demand parameters; EDPs), and $\mathcal{M}_{NLRHA}$ is the computational model. The input vector is typically represented as $\boldsymbol{X} = [\boldsymbol{X_G}, \boldsymbol{X_S}]$, where $\boldsymbol{X_G} \in \mathbb{R}^{n_G}$ corresponds to ground motion time histories and

$\boldsymbol{X_S} \in \mathbb{R}^{n_S}$ to structural parameters.

To address the challenges associated with high-dimensional uncertainty propagation and intensive computational cost, this study proposes a stochastic simulation framework that integrates physics-based dimensionality reduction with multivariate conditional distribution modeling. This framework enables efficient and accurate prediction of seismic responses while significantly reducing the number of required model evaluations. Furthermore, global sensitivity analysis (GSA) is performed by leveraging the trained stochastic simulator to quantify the relative contributions of aleatory and epistemic uncertainties. The proposed method is validated through application to a nonlinear finite element bridge model, demonstrating both accuracy and computational efficiency.

2 UNCERTAINTY QUANTIFICATION USING STOCHASTIC SIMULATION

2.1 Stochastic simulator model

The stochastic simulator is developed as a surrogate model that approximates the complex mapping from high-dimensional input variables to structural response quantities. The method consists of three key components:

- **Dimensionality reduction in input-output space:** Ground motion uncertainties are first mapped to a physics-informed representation using a set of spectral and intensity-based features. This is followed by a conventional dimensionality reduction algorithm, such as principal component analysis (PCA), applied to the augmented input-output space. The overall mapping is defined as:

$$\boldsymbol{\psi_z} = \mathcal{H}(\boldsymbol{x}, \boldsymbol{y}) = \mathcal{H}_r \circ \mathcal{H}_p(\boldsymbol{x}, \boldsymbol{y}) \tag{2}$$

  where

$$\mathcal{H}_p: \boldsymbol{x_G} \in \mathbb{R}^{n_G} \mapsto \boldsymbol{x'_G} \in \mathbb{R}^{n'_G} \tag{3}$$

$$\mathcal{H}_r: (\boldsymbol{x'_G}, \boldsymbol{x_S}, \boldsymbol{y}) \in \mathbb{R}^{n'_G + n_S + m} \mapsto \boldsymbol{\psi_z} \in \mathbb{R}^d \tag{4}$$

  Here, $\mathcal{H}_p$ maps ground motion time histories $\boldsymbol{x_G}$ to a reduced feature space $\boldsymbol{x'_G}$ using 109 spectral and intensity measures identified in [5]. $\mathcal{H}_r$ then performs further dimensionality reduction on the joint input-output space to produce a lower-dimensional representation $\boldsymbol{\psi_z}$. The reduced dimension d is selected using an iterative algorithm based on specified error threshold [5].

- **Conditional distribution modeling in reduced space:** Given the reduced feature $\boldsymbol{\psi_z}$, a multivariate conditional distribution $f_{\hat{Y}|\boldsymbol{\Psi_z}}$ is constructed to model the distribution of outputs conditioned on the reduced features. A kernel density estimation (KDE) model [6] is used for this purpose.

- **Stochastic simulation via transition kernel:** To perform probabilistic prediction, a transition kernel is defined over the reduced feature space. This kernel encodes the interplay between the dimensionality reduction mapping and the feature space conditional distribution. The resulting Markov chain converges to a stationary distribution, which is interpreted as the stochastic surrogate model:

$$T\left(\hat{\boldsymbol{y}}^{(t)}, \hat{\boldsymbol{y}}^{(t+1)} \middle| \boldsymbol{x}\right) = f_{\hat{Y}|\boldsymbol{\Psi}_z}\left(\hat{\boldsymbol{y}}^{(t+1)} \middle| \boldsymbol{\psi}_z\right) \cdot f_{\boldsymbol{\Psi}_z|\boldsymbol{XY}}\left(\boldsymbol{\psi}_z \middle| \boldsymbol{x}, \hat{\boldsymbol{y}}^{(t)}\right) \tag{5}$$

where $f_{\boldsymbol{\Psi}_z|\boldsymbol{XY}}\left(\boldsymbol{\psi}_z \middle| \boldsymbol{x}, \hat{\boldsymbol{y}}^{(t)}\right)$ is determined through the mapping $\mathcal{H}$ in Eqs. (2)-(4). After discarding burn-in period, the resulting sequence $\hat{\boldsymbol{y}}^{(t)}$ from $t = n_b + 1$ to n_t provides a stochastic approximation to the model response for a given input $\boldsymbol{x}$. The parameters n_b and n_t denote the number of burn-in samples and total iterations, respectively.

2.2 Forward uncertainty quantification

The stochastic simulator enables forward UQ by generating random samples of structural responses conditioned on a given input $\boldsymbol{x}$. Using a sequence of random vectors generated by transition kernel, key statistical quantities, including the mean vector and covariance matrix, are computed as follows:

$$\boldsymbol{\mu}_{\hat{Y}}(\boldsymbol{x}) = \frac{1}{n_t - n_b} \sum_{t=n_b+1}^{n_t} \hat{\boldsymbol{y}}^{(t)} \tag{6}$$

$$\boldsymbol{\Sigma}_{\hat{Y}\hat{Y}}(\boldsymbol{x}) = \frac{1}{n_t - n_b - 1} \sum_{t=n_b+1}^{n_t} \left(\hat{\boldsymbol{y}}^{(t)} - \boldsymbol{\mu}_{\hat{Y}}\right)\left(\hat{\boldsymbol{y}}^{(t)} - \boldsymbol{\mu}_{\hat{Y}}\right)^T \tag{7}$$

The diagonals of covariance matrix represent the marginal variances of individual EDP, while the off-diagonal terms reflect the pairwise correlations between EDPs. This allows a direct quantification of uncertainty in seismic demand parameters.

2.3 Global sensitivity analysis

The stochastic simulator is further applied to variance-based GSA using Sobol' indices [7]. This method quantifies the contribution of each uncertainty source to the variance in structural responses. Grouped sensitivity indices are computed with respect to the input groups $\boldsymbol{X_G}$ and $\boldsymbol{X_S}$. For the *k*-th output Y_k, the first-order Sobol' index for $\boldsymbol{X_G}$ is given by:

$$S_{\boldsymbol{G}}^{k} = \frac{\mathbb{V}\mathrm{ar}_{\boldsymbol{X_G}}\left[\mathbb{E}_{\boldsymbol{X}_{\sim \boldsymbol{G}}}[Y_k|\boldsymbol{X_G}]\right]}{\mathbb{V}\mathrm{ar}[Y_k]} \tag{8}$$

where $\boldsymbol{X}_{\sim\boldsymbol{G}}$ denotes all inputs excluding $\boldsymbol{X_G}$, and $\mathbb{E}_{\boldsymbol{X}_{\sim\boldsymbol{G}}}$ represents the conditional expectation over $\boldsymbol{X}_{\sim\boldsymbol{G}}$. The corresponding index for structural parameters $S_{\boldsymbol{S}}^{k}$ can be computed by replacing $\boldsymbol{X_G}$ with $\boldsymbol{X_S}$ in Eq. (8).

Due to the high-dimensionality of the input space, direct computation of Sobol' indices using standard MCS is computationally infeasible. The proposed framework circumvents this issue by replacing full NLRHA evaluations with the stochastic simulator, and applying stratified MCS [8]. Note that grouped Sobol' indices provide insights into the dominant contributors to seismic response variability in terms of ground motion variability and structural parameter uncertainties.

The overall framework for forward UQ and GSA using the proposed stochastic simulator is illustrated in Figure 1.

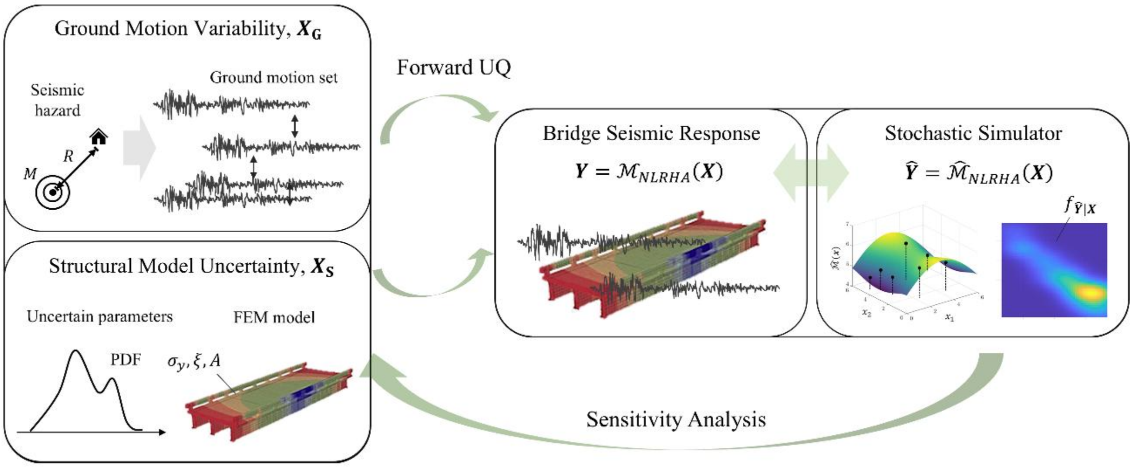

Figure 1: Stochastic simulation framework for forward uncertainty quantification and global sensitivity analysis of bridge responses, incorporating ground motion variability and structural parameter uncertainty

3 CASE STUDIES: BRIDGE APPLICATIONS

The proposed framework is applied to a representative bridge structure designed by Caltrans—the Auburn Ravine Bridge, a prestressed concrete girder bridge consisting of six spans and two piers per bent [9]. The finite element model is developed in OpenSees [10] and accounts for nonlinear behavior.

3.1 Input and output dataset

The FE model of the Auburn Ravine bridge is shown in Figure 2. Structural uncertainties include material properties (e.g., concrete compressive strength, reinforcement yield strength), geometric characteristics (e.g., pier dimensions), and damping ratios. These are summarized in Table 1. In this table, parameters P_1 and P_2 denote the lower and upper bounds for uniform distributions, and the mean and coefficient of variation for lognormal distributions.

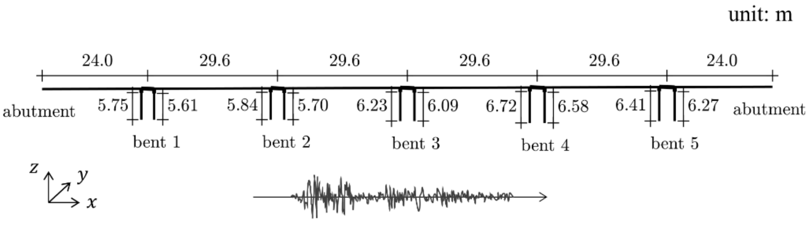

Figure 2: Auburn Ravin bridge finite element model

Ground motion input consists of 2,000 recorded accelerograms selected from the PEER NGA-West2 database [11], consistent with hazard parameters from a ground motion model [12] assuming a moment magnitude of 6.5, rupture distance of 10 km, average shear-wave velocity of 450 m/s, and a normal fault type. Using the ground motion selection algorithm from [13], these records were selected to be spectrum-compatible. Paired with samples of structural parameter realizations, this yields a dataset of 2,000 input-output samples.

Table 1: Uncertain structural parameters in the Auburn Ravin bridge model

Bridge parameter	P_1	P_2	Distribution
Damping ratio	0.05	0.35	Lognormal
Area of girder cross-section (m^2)	4.50	8.50	Uniform
Elastic modulus of girder (MPa)	28300	0.35	Lognormal
Elastic modulus of pier steel (MPa)	200000	0.35	Lognormal
Yield strength of pier steel (MPa)	475	0.35	Lognormal
Ultimate strength of pier steel (MPa)	655	0.35	Lognormal
Onset of hardening strain	0.0115	0.30	Lognormal
Elastic modulus of pier concrete (MPa)	27600	0.30	Lognormal
Compressive strength of pier concrete (MPa)	34.5	0.30	Lognormal
Strain at compressive strength	0.002	0.25	Lognormal
Diameter of pier column (m)	0.90	1.90	Uniform
Thickness of concrete cover (m)	0.02	0.08	Uniform

3.2 Forward UQ results

For forward UQ analysis, the simulator is applied to predict the peak flexural bending moments M_y and M_z for each of the 25 girders. A total of 700 samples is used to train the simulator. Dimensionality is reduced to $d = 27$, and the conditional distribution is modeled using a multivariate KDE approach with 7 mixture components.

Figure 3 presents the marginal probability density functions (PDFs) of selected girder bending moments, comparing predictions from the stochastic simulator against reference MCS results. Solid lines represent the MCS reference, and dashed lines indicate the simulator predictions, confirming strong agreement in both central tendency and dispersion.

Figure 4 displays the Pearson correlation coefficient matrices across the 25 girders. The axes correspond to girder indices ordered longitudinally from the left to the right abutment. These results highlight the simulator's ability to accurately reproduce the interdependencies among multivariate responses while significantly reducing the computational cost.

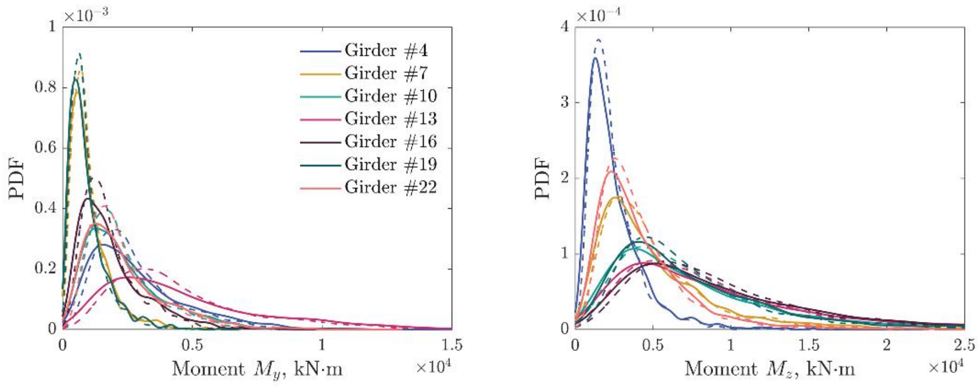

Figure 3: Marginal PDFs of bending moments M_y and M_z for selected girders

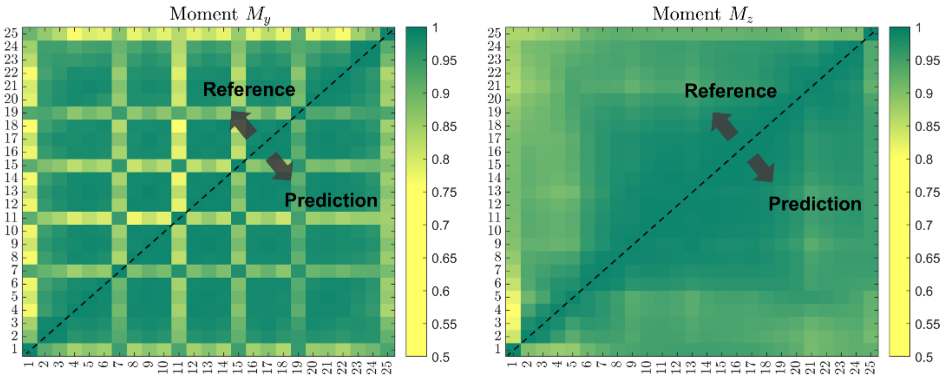

Figure 4: Correlation matrices of girder bending moments M_y and M_z

3.3 Sensitivity analysis results

Using the simulator trained in Section 3.2, variance-based global sensitivity analysis is conducted as described in Section 2.3. Figure 5 shows the first-order Sobol' indices for the 25 girder's bending moments, including contributions from ground motion uncertainties, structural parameter uncertainties, and their interaction effects, computed as $S_{\boldsymbol{S,G}}^k = 1 - S_{\boldsymbol{S}}^k - S_{\boldsymbol{G}}^k$. Each plot includes reference values (solid lines), stochastic simulator prediction means (dashed lines), and 95% confidence intervals (shaded areas) for 25 girder responses.

Results indicate that ground motion uncertainty dominates the variability in girder responses, contributing more than 60% of the total variance. Structural parameter uncertainties contribute up to 30%, especially in locations where structural stiffness significantly affects dynamic response. Spatial variations in sensitivity are evident along the bridge deck, demonstrating the simulator's capacity to resolve localized effects. These findings confirm that the proposed stochastic simulator can reliably reproduce response variability and its sensitivity to high-dimensional uncertainties, with substantially lower computational cost than traditional MCS.

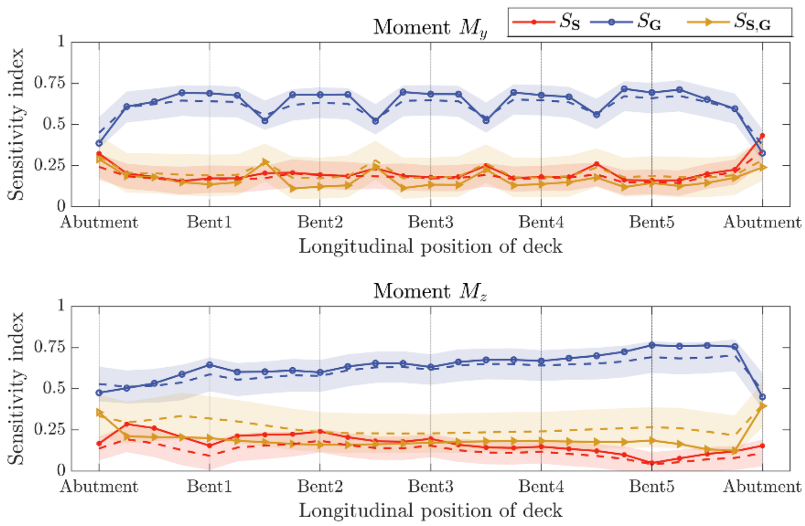

Figure 5: Sobol' indices for girder bending moments, showing contributions from ground motion, structural parameters, and their interaction along the deck

4 CONCLUSIONS

This study presented a stochastic modeling framework for UQ and sensitivity analysis of seismic responses in bridge structures. The proposed method integrates physics-based dimensionality reduction with probabilistic modeling to construct a stochastic simulator capable of efficiently propagating high-dimensional input uncertainties. Forward UQ analysis was conducted to estimate the marginal distributions and correlations of EDPs, while variance-based global sensitivity analysis quantified the relative contributions of aleatory and epistemic uncertainties. The framework was validated through application to a realistic nonlinear finite element bridge model, demonstrating both high predictive accuracy and significant computational savings. Results indicated that aleatory uncertainties from ground motions are the dominant source of seismic response variability, though epistemic uncertainties related to structural parameters remain influential. These findings offer practical insights for seismic design, enabling targeted treatment of uncertainty sources, and support performance-based engineering and risk-informed decision-making for bridge infrastructure. Future research will explore extensions of this framework to optimization-based decision-making and resilience assessment [14,15].

ACKNOWLEDGMENTS

This research was supported by the Pacific Earthquake Engineering Research Center grant NCTRZW. This research was also supported by the Basic Science Research Program through the National Research Foundation of Korea (NRF) funded by the Ministry of Education (RS-2024-00407901).

REFERENCES

[1] Yi, S. R., and Taflanidis, A. A. (2025). Multi-output stochastic emulation with applications to seismic response correlation estimation. *Structural Safety*, 102578.

[2] Günay, S., and Mosalam, K. M. (2013). PEER performance-based earthquake engineering methodology, revisited. *Journal of Earthquake Engineering*, 17(6), 829-858.

[3] Kim, J., Wang, Z., and Song, J. (2024). Adaptive active subspace-based metamodeling for high-dimensional reliability analysis. *Structural Safety*, 106, 102404.

[4] Kim, J., Yi, S. R., and Wang, Z. (2024). Dimensionality reduction can be used as a surrogate model for high-dimensional forward uncertainty quantification. *arXiv preprint* arXiv:2402.04582.

[5] Kim, J., and Wang, Z. (2025). Uncertainty quantification for seismic response using dimensionality reduction-based stochastic simulator. *Earthquake Engineering & Structural Dynamics*, 54(2), 471-490.

[6] Kristan, M., Leonardis, A., and Skočaj, D. (2011). Multivariate online kernel density estimation with Gaussian kernels. *Pattern recognition*, 44(10-11), 2630-2642.

[7] Saltelli, A., Ratto, M., Andres, T., Campolongo, F., Cariboni, J., Gatelli, D., Saisana, M., and Tarantola, S. (2008). *Global sensitivity analysis: the primer*. John Wiley & Sons.

[8] Saltelli, A., Annoni, P., Azzini, I., Campolongo, F., Ratto, M., & Tarantola, S. (2010). Variance based sensitivity analysis of model output. Design and estimator for the total sensitivity index. *Computer physics communications*, 181(2), 259-270.

[9] Konakli, K., & Der Kiureghian, A. (2012). Simulation of spatially varying ground motions

including incoherence, wave-passage and differential site-response effects. *Earthquake Engineering & Structural Dynamics*, 41(3), 495-513.

[10] McKenna, F. (2011). OpenSees: a framework for earthquake engineering simulation. *Computing in Science & Engineering*, 13(4), 58-66.

[11] Ancheta, T. D., Darragh, R. B., Stewart, J. P., Seyhan, E., Silva, W. J., Chiou, B. S. J., Wooddell, K.E., Graves, R.W., Kottke, A.R., Boore, D.M., and Donahue, J. L. (2014). NGA-West2 database. *Earthquake Spectra*, 30(3), 989-1005.

[12] Campbell, K. W., & Bozorgnia, Y. (2014). NGA-West2 ground motion model for the average horizontal components of PGA, PGV, and 5% damped linear acceleration response spectra. *Earthquake Spectra*, 30(3), 1087-1115.

[13] Baker, J. W., & Lee, C. (2018). An improved algorithm for selecting ground motions to match a conditional spectrum. *Journal of Earthquake Engineering*, 22(4), 708-723.

[14] Kim, J., Yi, S. R., and Song, J. (2024). Active learning-based optimization of structures under stochastic excitations with first-passage probability constraints. *Engineering Structures*, 307, 117873.

[15] Kim, J., Yi, S. R., Park, J., and Kim, T. (2024). Efficient system reliability–based disaster resilience analysis of structures using importance sampling. *Journal of Engineering Mechanics*, 150(11), 04024081.